Run I Legacy Performance : electrons/ photons (ATLAS)

by Denis Oliveira Damazio
on behalf of the ATLAS Collaboration

In this talk, the run 1 legacy performance of the electron and photon reconstruction and identification in the ATLAS and CMS experiments will be described, as well as the associated systematic uncertainties. The two speakers should try to enlight the differences of performances between the two experiments, and explain what worked better/worse than planned, as well as the lessons for the run 2.

The ATLAS detector

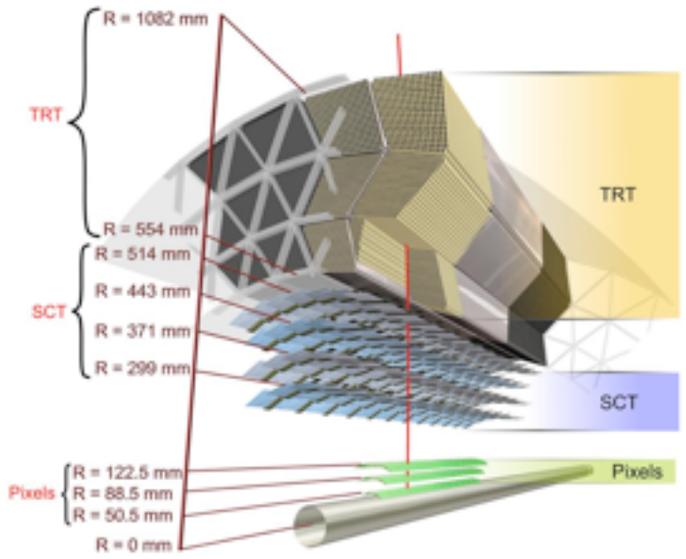

- ATLAS is equipped with highly segmented tracking detectors :
  - Pixels 3 layers, 80 million channels.
  - SemiConductor Tracker : 4 layers with double sided readout.
  - Transition Radiation Tracker (up to 35 measurements per track). Able to perform electron/pion separation.
- A 2T magnetic field around tracker.
- A fine granularity lead-liquid argon electromagnetic calorimeter contributes with precise shower shape measurement to particle classification.
- Hadronic calorimeters (for fake electron/photon veto'ing).
- Electron/photon reconstruction are fundamental for Higgs, Standard Model precision physics and a variety of studies.

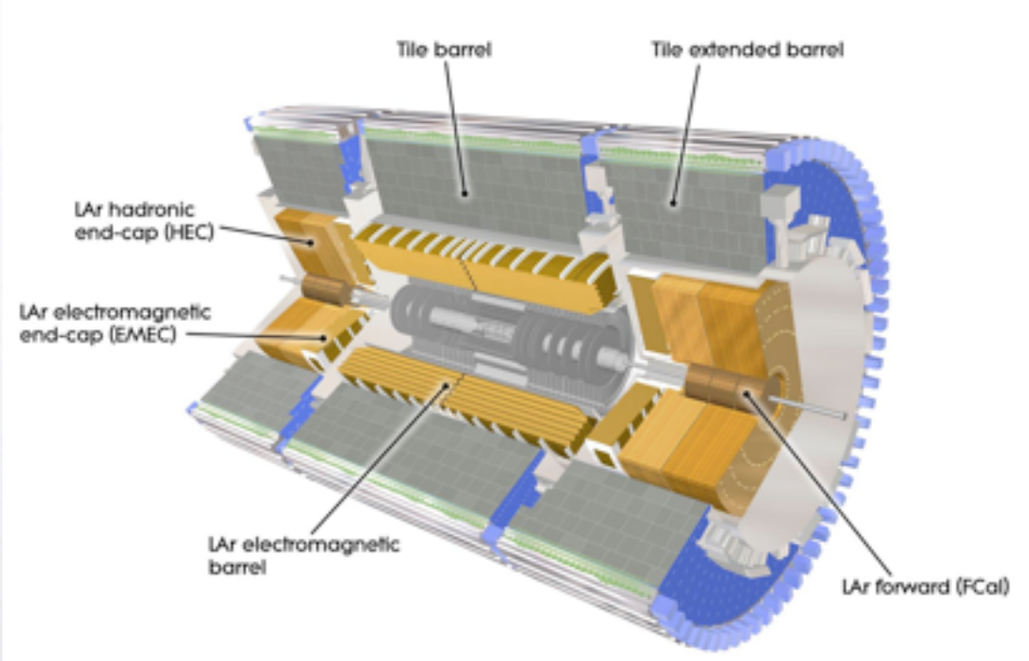

Electron and photon reconstruction

- A minimal (δ η, δ Φ)=(0.075,0.125) EM Calorimeter grid 2.5 GeV (local maximum) is required to become a cluster seed : sliding window algorithm
- Tracks loosely matched to the cluster are used to build electron candidates. Pattern recognition improvements and refitting the tracks with the Gaussian Sum Filter (based on Kalman filtering to account for bremsstrahlung energy loss in the inner detector) resulted in an important performance improvement in 2012.
- Possible converted photon candidates are reconstructed in the same manner : Loosely matched tracks help on vertex finding.
- Unconverted photon candidates are formed from clusters only.
- Position corrections and energy calibration optimized per particle type can be applied.

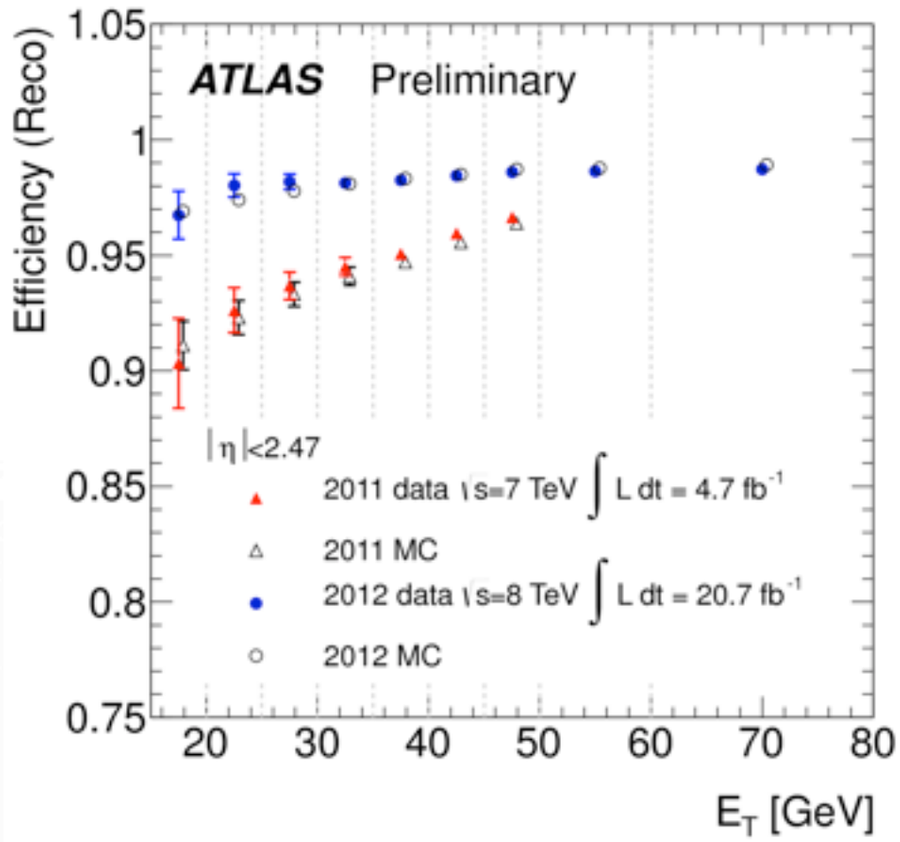

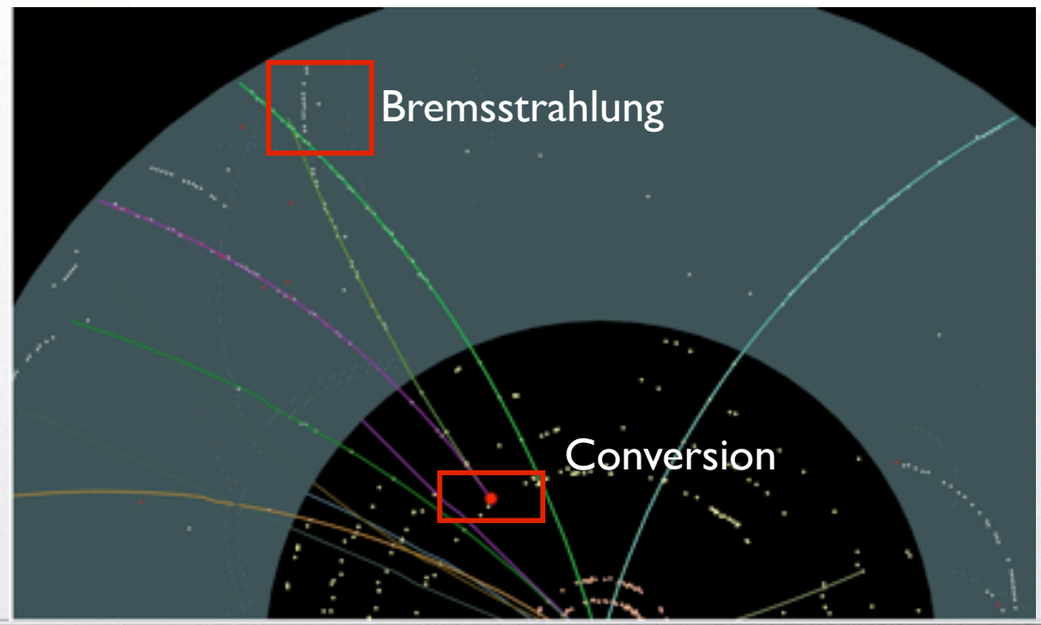

E/gamma identification

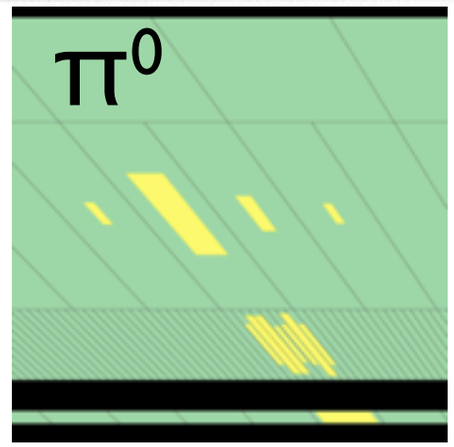

- Cluster variables used for central photons identification. For electrons, track quality, TRT fraction and cluster-track matching also included (all variables in backup).
- Cuts performed on these variables allow to identify electron, converted and unconverted photons.
- Different operating points translating to different levels of purity : loose, medium, tight. Cuts are optimized in 2D (η,E_T) bins.
- For 2012 electrons, possibility of using Likelihood (product of PDFs of discriminating variables from signal and background samples).
- Forward electrons ($2.5 < |\eta| < 4.9$) do not have tracking : cluster moments are used (backup).

Variables and Position

	Strips	2nd	Had.
Ratios	f_1, f_{side}	R_η*, R_ϕ	$R_{Had.}$*
Widths	$w_{s,3}$, $w_{s,tot}$	$w_{\eta,2}$*	-
Shapes	ΔE, E_{ratio}	* Used in PhotonLoose.	

Energy Ratios

$R_\eta = \frac{E^{S2}_{3\times7}}{E^{S2}_{7\times7}}$ $R_\phi = \frac{E^{S2}_{3\times3}}{E^{S2}_{3\times7}}$

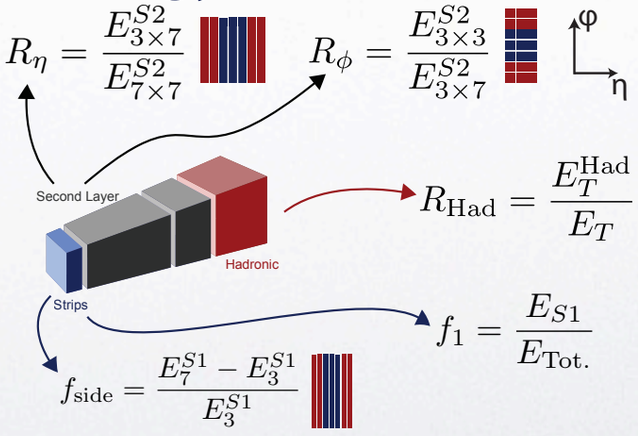

$R_{\mathrm{Had}} = \frac{E_T^{\mathrm{Had}}}{E_T}$

$f_1 = \frac{E_{S1}}{E_{\mathrm{Tot.}}}$

$f_{\mathrm{side}} = \frac{E^{S1}_7 - E^{S1}_3}{E^{S1}_3}$

Shower Shapes

$E_{\mathrm{ratio}} = \frac{E^{S1}_{\mathrm{max},1} - E^{S1}_{\mathrm{max},2}}{E^{S1}_{\mathrm{max},1} + E^{S1}_{\mathrm{max},2}}$

$\Delta E = E^{S1}_{\mathrm{max},2} - E^{S1}_{\mathrm{min}}$

Widths

$w_{\eta,2} = \sqrt{\frac{\sum E_i \eta_i^2}{\sum E_i} - \left(\frac{\sum E_i \eta_i}{\sum E_i}\right)^2}$

Width in a 3×5 (Δη×Δφ) region of cells in the second layer.

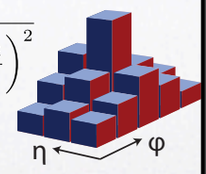

$w_s = \sqrt{\frac{\sum E_i (i - i_{\mathrm{max}})^2}{\sum E_i}}$

ws3 = w_1 uses 3 strips in η; wstot is defined similarly, but uses 20 strips.

Likelihood discriminant :

$$d_{\mathcal{L}} = \frac{\mathcal{L}_S}{\mathcal{L}_S + \mathcal{L}_B}, \qquad \mathcal{L}_S(\vec{x}) = \prod_{i=1}^{n} P_{s,i}(x_i)$$

Electron efficiency measurement

- Tag and Probe methods based on J/ψ, Z->ee,W->eν (2011) and Z->ee γ (2012) are used to cover a large fraction of the E_T range.
- For each E_T and η bin background templates are obtained prior and after ID selection (for the three operating points in 2011, more in 2012 - see ahead) by reversing some of the ID cuts.
- Templates are scaled in side-bands so that efficiency can be obtained with simple formula below in the signal region.
- Systematics are obtained by varying conditions to build templates, mass windows, cut tightness, etc.
- Efficiencies with the same reconstruction and identification cuts are determined for MC using truth matching.
- Low E_T probes (bottom picture) particularly harder to evaluate efficiency and errors.

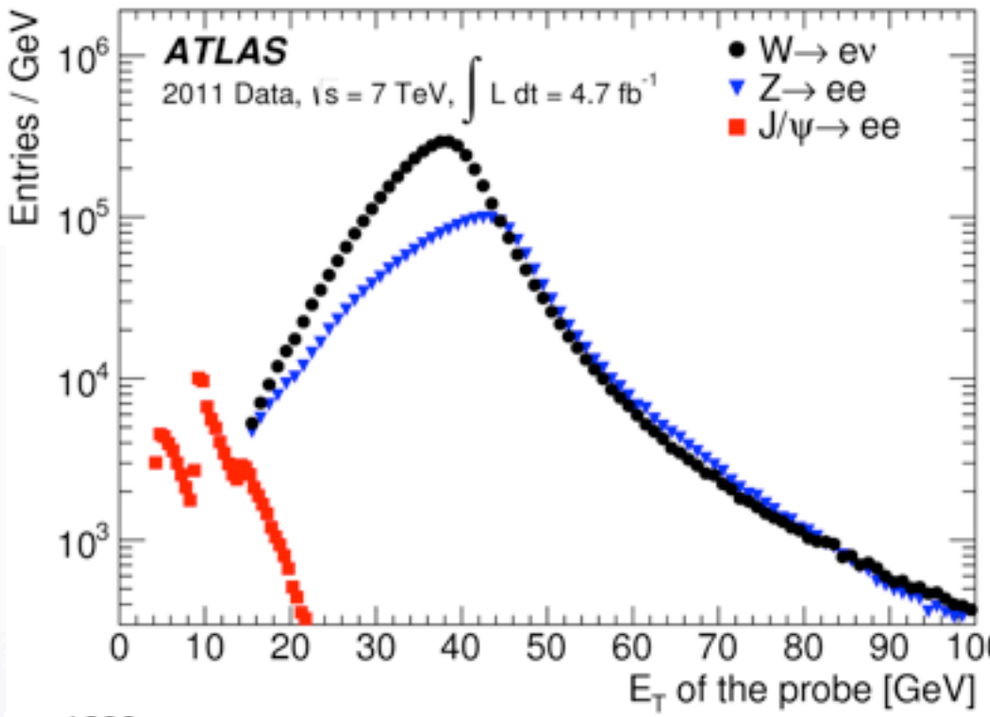

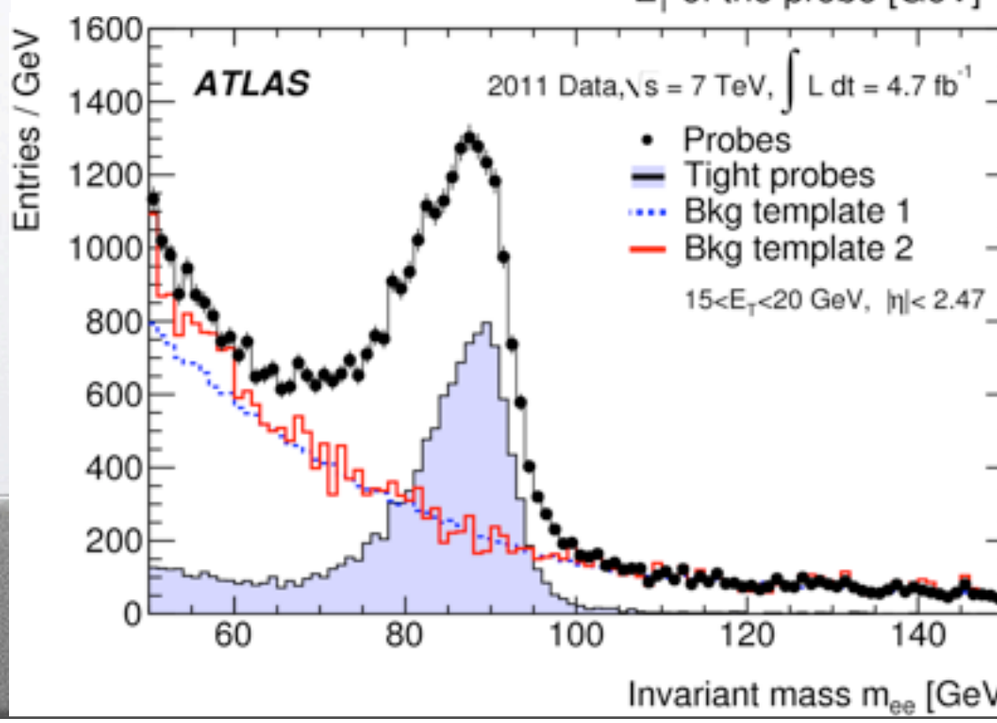

$$\frac{\text{number of probes passing ID in signal region - background template for ID}}{\text{number of all probes in signal region - background template}}$$

Electron efficiency results - 2011

- Efficiencies are obtained in bins of E_T and η (only E_T shown here).
- Measurements also performed with respect to the number of primary vertices (pile-up).
- Total uncertainty in efficiency is 0.1% at 35 GeV, reaching 1-2% for lower E_T. Data-to-MC scale factors normally close to 1, but deviating a few percent at low E_T or high η.

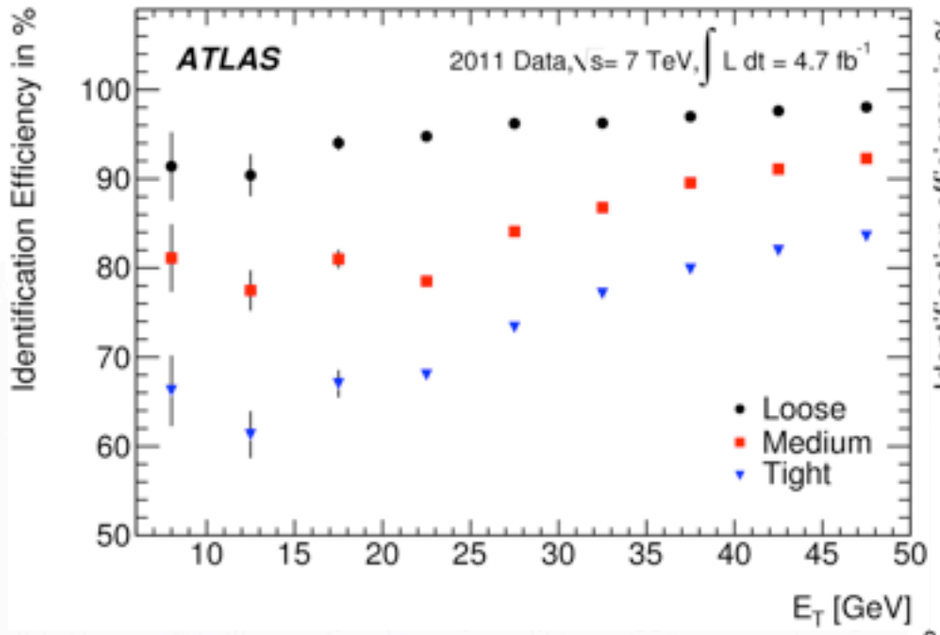

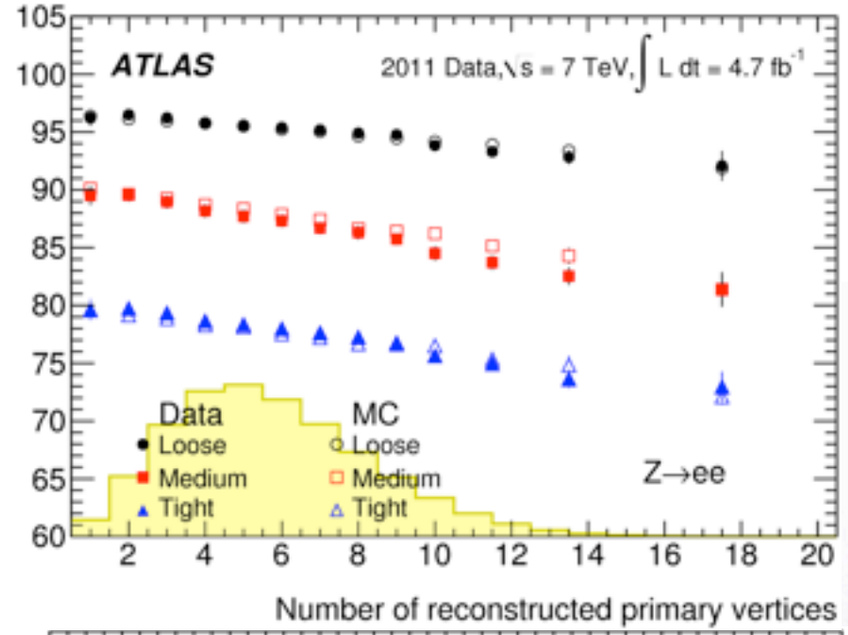

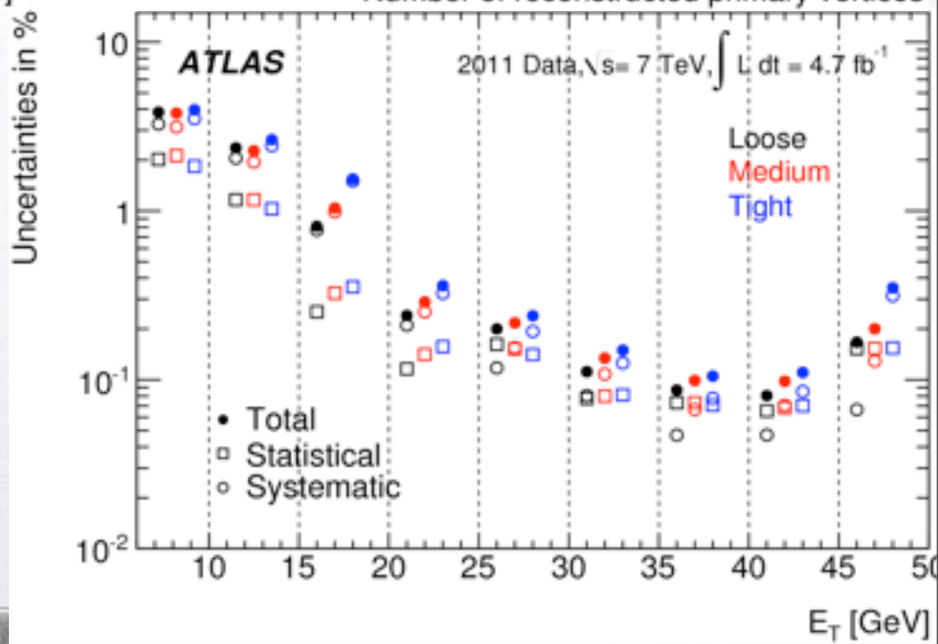

Electron reconstruction and identification efficiency measurements with the ATLAS detector using the 2011 LHC proton--proton collision data

Electron efficiency results -2012

- In 2012, for each cut based operating point, a Likelihood one was also included. Also, a new Multilepton point included for cut-based. Efficiency evaluated in 2D bins (η,E_T).
- Higher stability with respect to the number of primary vertices (see backup for comparison 2011/2012) thanks to large effort to depend less on the variables more sensitive to pile-up.
- Preliminary total uncertainty on identification is around 5-6% (1-2%) for electrons below (above) E_T=25 GeV. Data-to-MC scale factors normally close to 1.

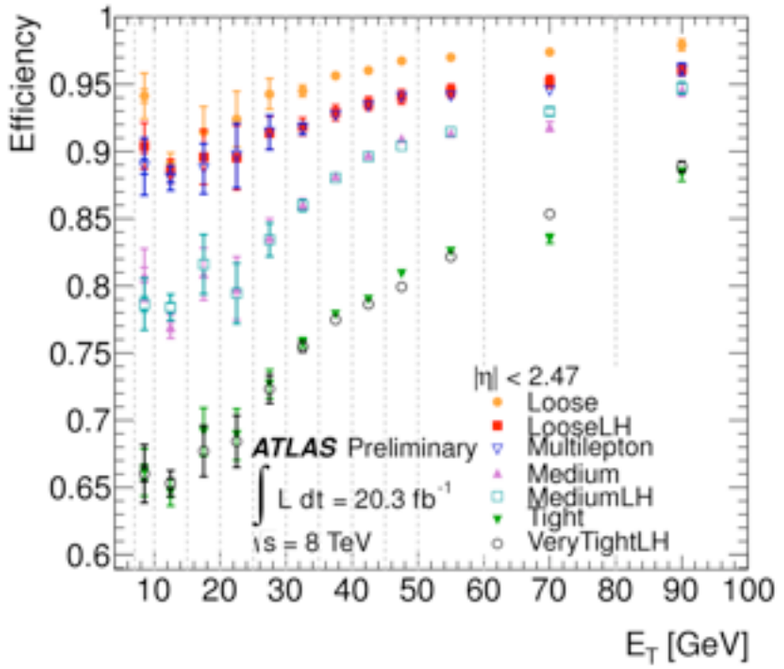

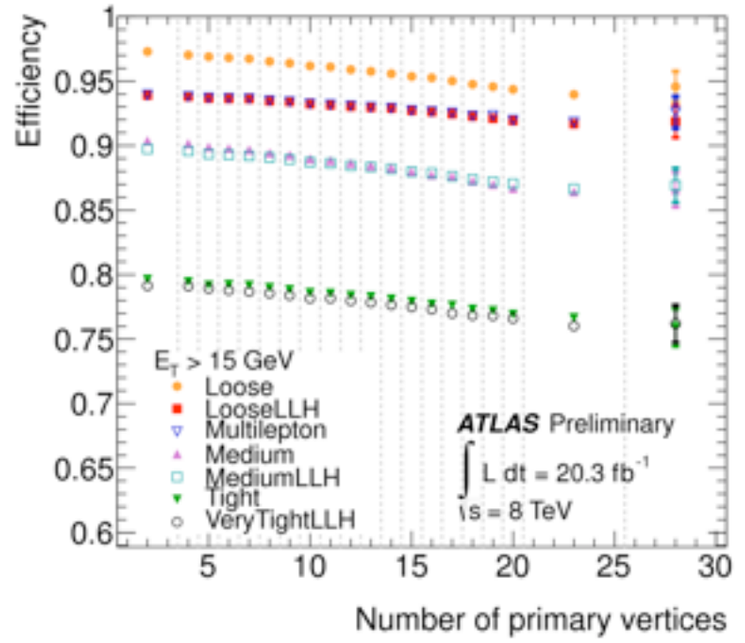

- Efficiency for LH operating points was made to match cut based ones whilst keeping factor of ~2 reduction in background (increased purity) : big impact in H->4e sensitivity.

Background efficiency improvement with LH over cut-based

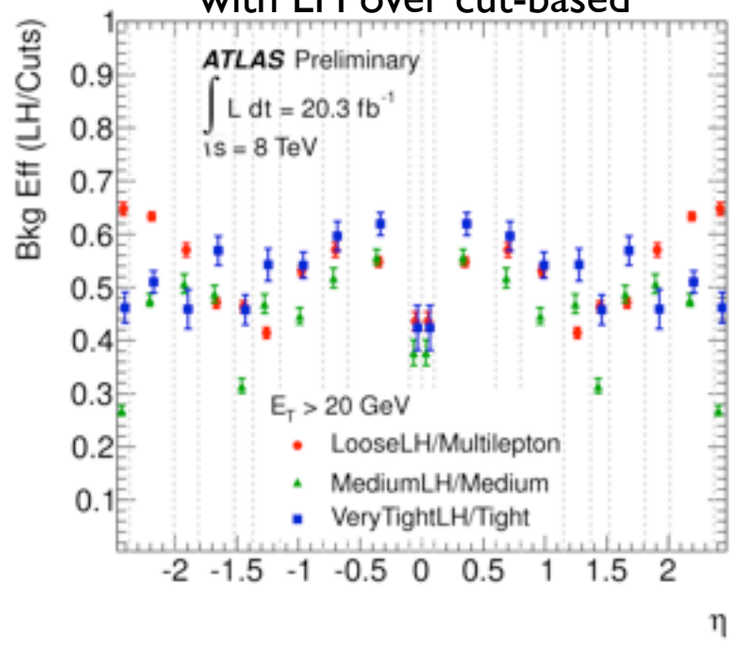

Electron efficiency measurements with the ATLAS detector using the 2012 LHC proton-proton collision data

Photon efficiency measurement

- Three methods for photon efficiency :
  - Z->ee tag-and-probe provide a clean sample of electrons, from which an extrapolation to photons using MC differences can be performed.
  - Z->ll γ decays (low stats) : two tags/one probe.
  - Matrix method : measure the tight/loose identification efficiency using isolation to subtract background in the loose probe (works best at high E_T where purity of loose photons is better).
- Here, brief discussion on Electron extrapolation. See other methods in backup.
- Smirnov transform on Cumulative Distribution Function (CDF) on MC samples map electron->photons.
- Performance evaluated in "transformed electrons" sample.

Electron extrapolation

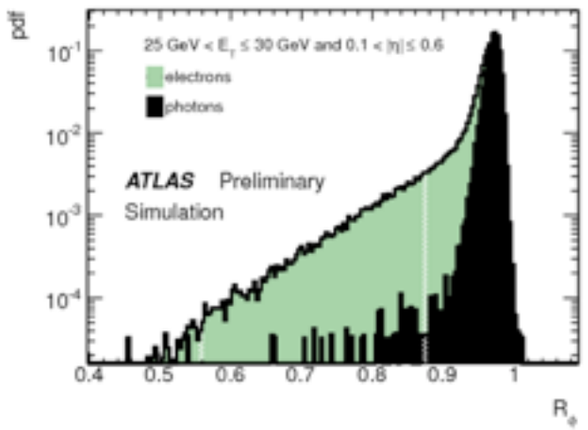

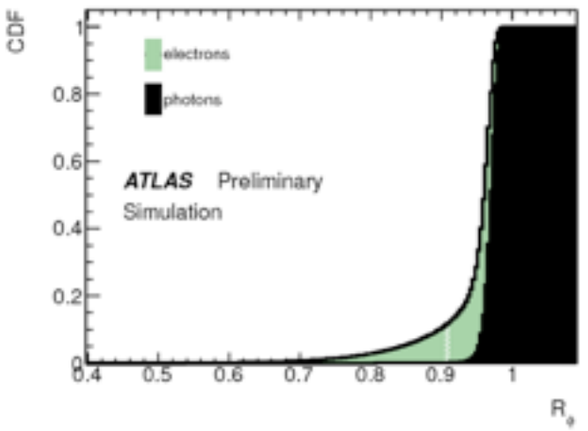

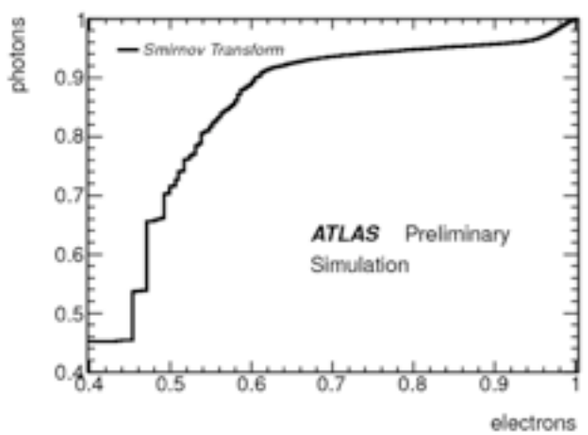

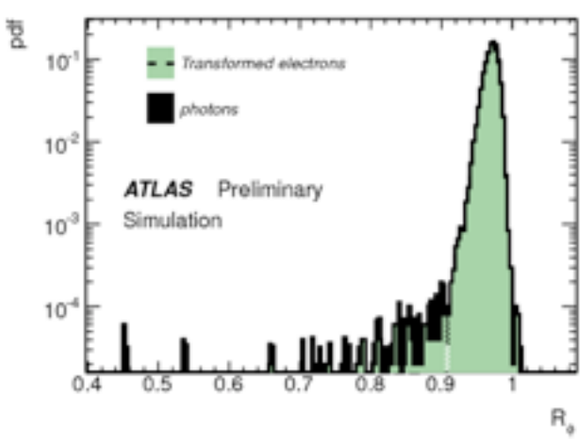

Photon efficiency results -2012

- Only cut based ID methods applied to photons.
- Here, only unconverted photons (see converted in backup).
- The methods agree well within their error bars where they overlap.
- Given the independent nature of the methods (and samples!), the results can be combined.
- 1-1.5 (0.5)% total uncertainty for photons below (above) 50 GeV.

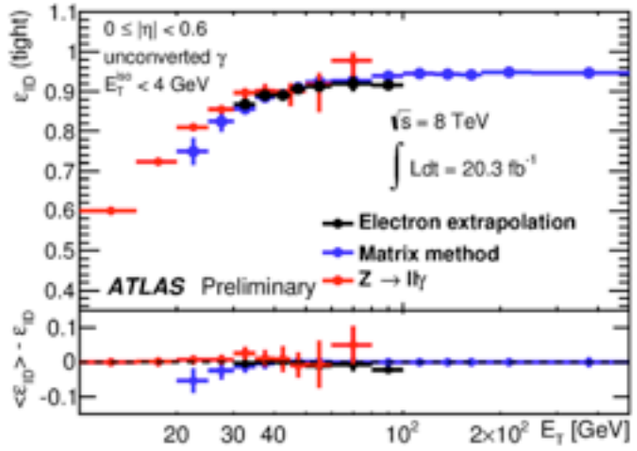

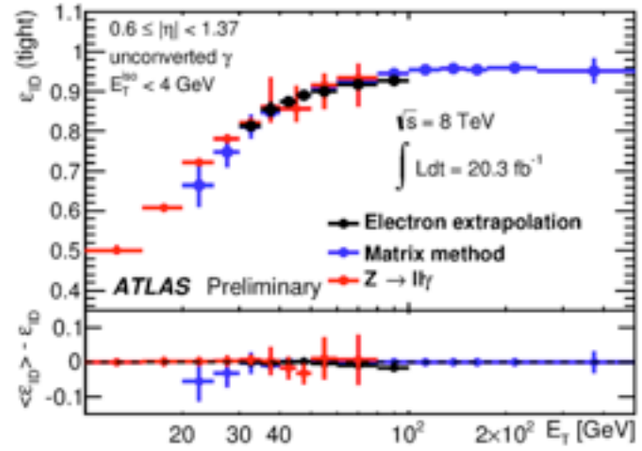

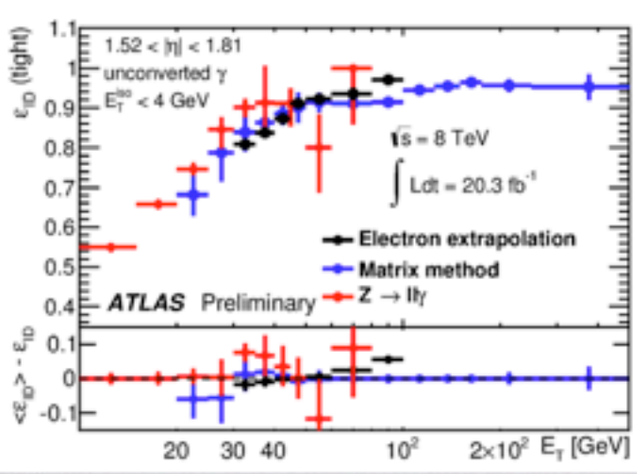

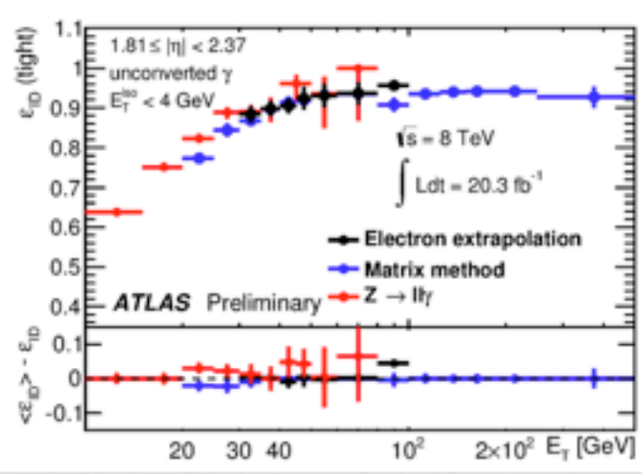

Measurements of the photon identification efficiencies using 20.3 fb^{-1} of pp collisions collected by ATLAS at √s = 8 TeV in 2012.

Improvements for 2015

- A new pixel layer (Insertable B-layer, IBL) was installed for Run2 directly on the beam pipe (with 3.2 cm radius), also uses 3d sensors.
- 14 M readout channels in IBL in addition to 80 M in current pixel detector.
- Reconstruction and identification will have to be adapted to IBL and expected Run 2 running conditions (pileup, 25 ns bunch spacing, …)

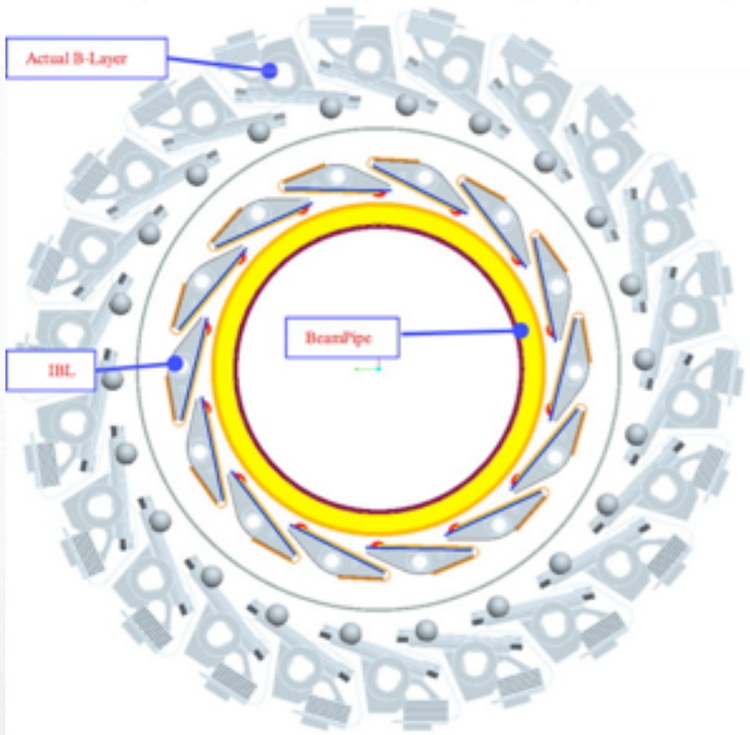

Conclusions

- Excellent performance of the detector for reconstruction and identification of electrons and photons.
- Different efficiency measurement techniques applied to ensure good knowledge of detector/reconstruction/identification performance.
- Improvements in calibration (MVA-based, see backup), reconstruction (in particular in tracking), better material description, more robust cut tuning and Likelihood identification had important impact in 2012 performance.
- New calibration later applied to 2011 dataset.
- These experiences plus new IBL will drive our reconstruction and identification performance in 2015.

References

- 2012 performance papers/notes :
  - ***Electron efficiency measurements with the ATLAS detector using the 2012 LHC proton-proton collision data***
  - ***Measurements of the photon identification efficiencies using 20.3 fb^{-1} of pp collisions collected by ATLAS at $\sqrt{s}$ = 8 TeV in 2012***.
  - Electron and photon energy calibration with the ATLAS detector using LHC Run 1 data
- 2011 longer papers/notes :
  - Electron reconstruction and identification efficiency measurements with the ATLAS detector using the 2011 LHC proton--proton collision data
  - ***Measurements of the photon identification efficiency with the ATLAS detector using 4.9 fb−1 of pp collision data collected in 2011***
- Expected Performance or earlier papers :
  - Electron performance measurements with the ATLAS detector using the 2010 LHC proton-proton collision data
  - ***Expected electron performance in the ATLAS experiment***
  - ***Expected photon performance in the ATLAS experiment***

backup

Possibly relevant information

- Material in front of the calorimeter : usage in calibration and ID discussions. Improved knowledge since 2012.
- Luminosity provided by LHC constantly challenging detectors.

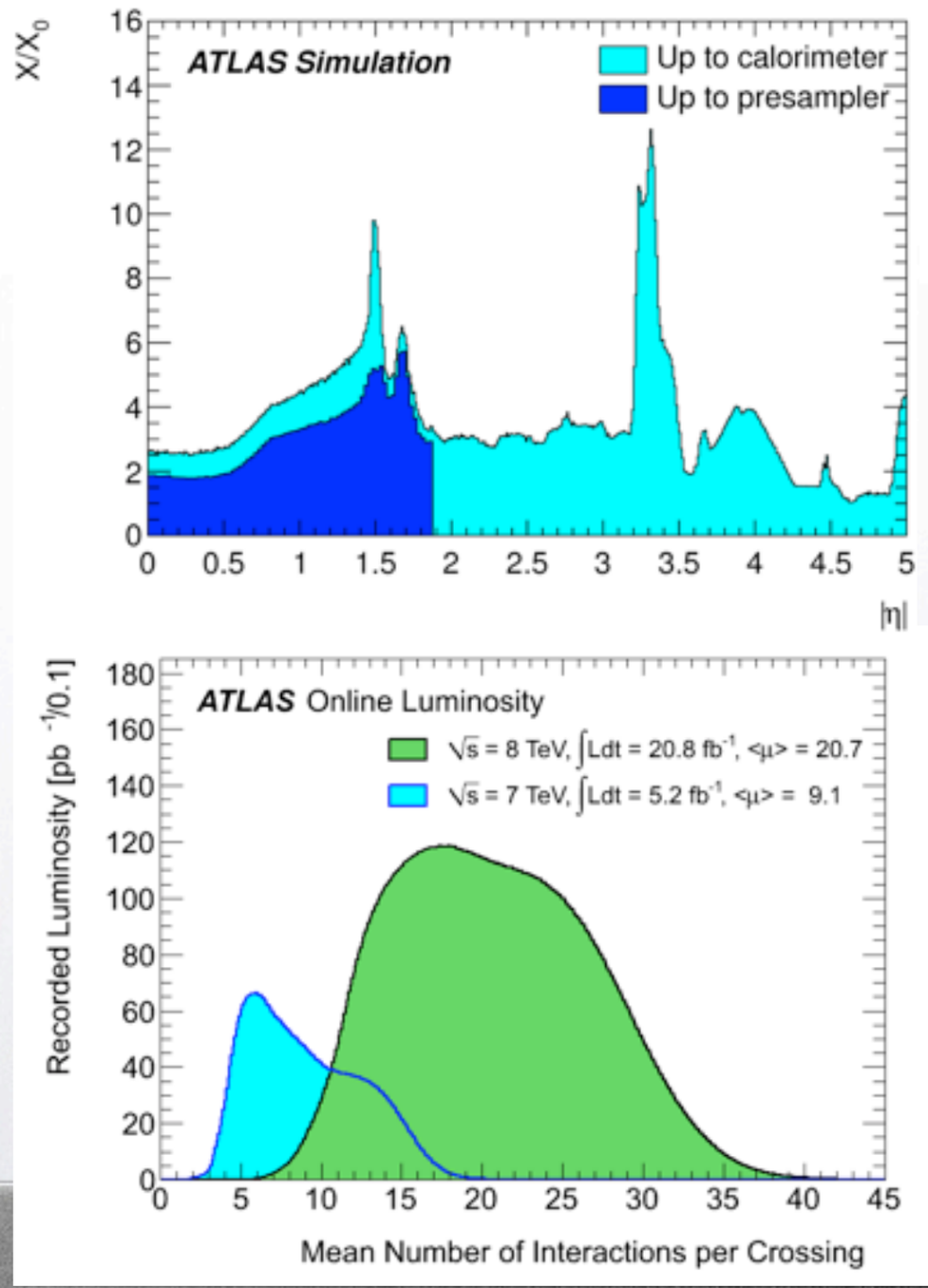

Using Z->llγ

- Technique for photon identification performance measurement.
- Lower statistics in 2011.
- Studying the decays in a pair of electrons or muons and a photon.
- Background templates also defined by reverting cuts.
- Also used for electron efficiency for E_T=10-15 GeV using tight photon probe (2012).

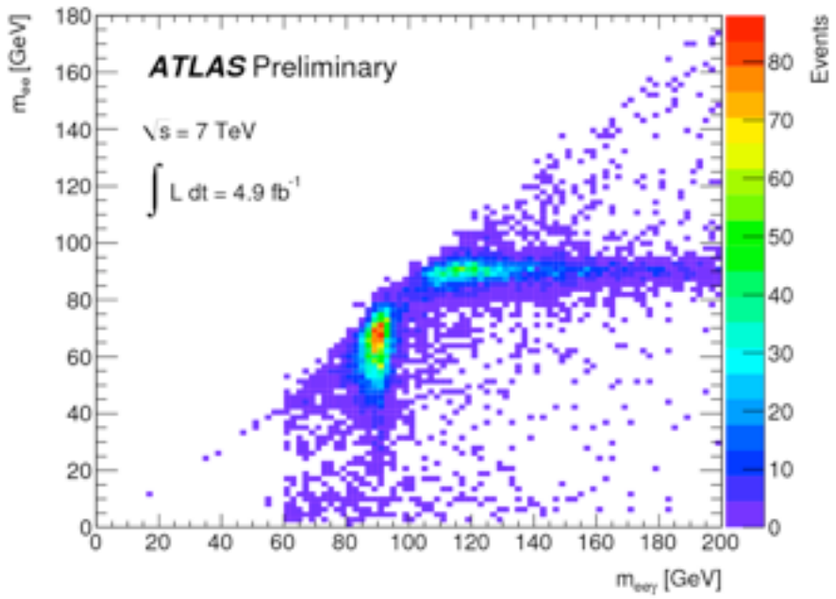

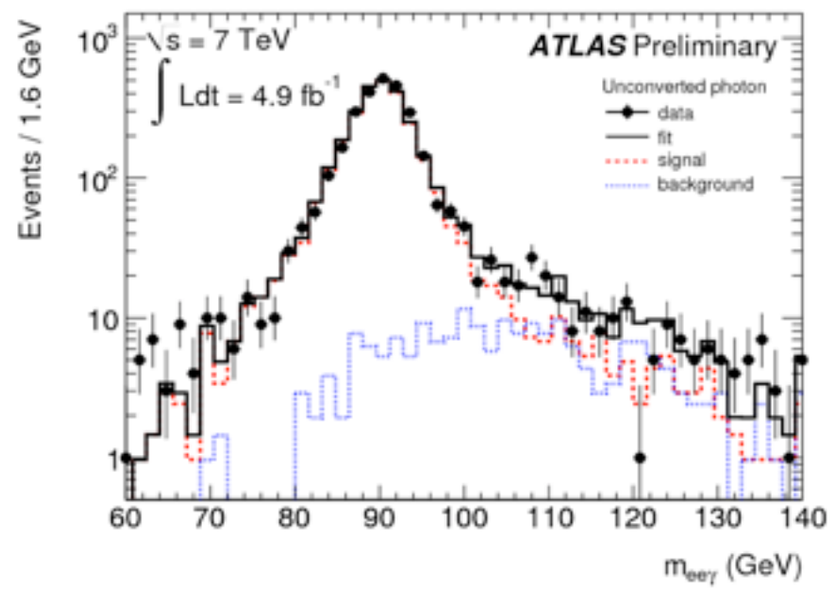

Matrix method

- Technique for photon identification performance measurement.
- Selecting a number of (assumed) uncorrelated cuts, and measuring the photon purity of a MC sample before after a different selection, one can measure the purity in the difference (1,2,3,4) regions.
- The same purities can be applied to a data sample and result in efficiency measurement.

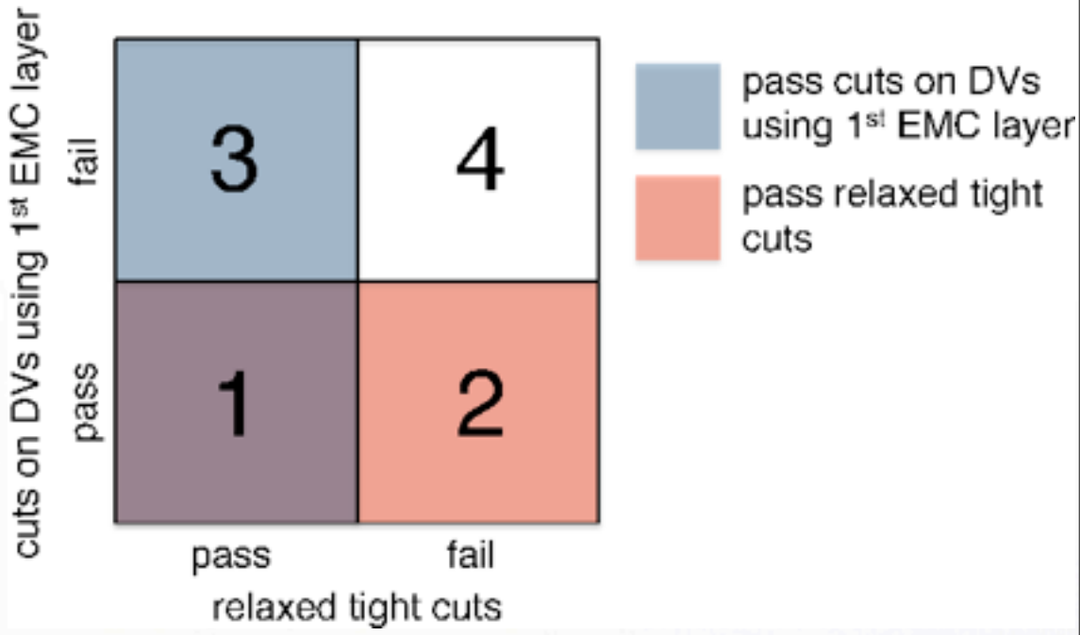

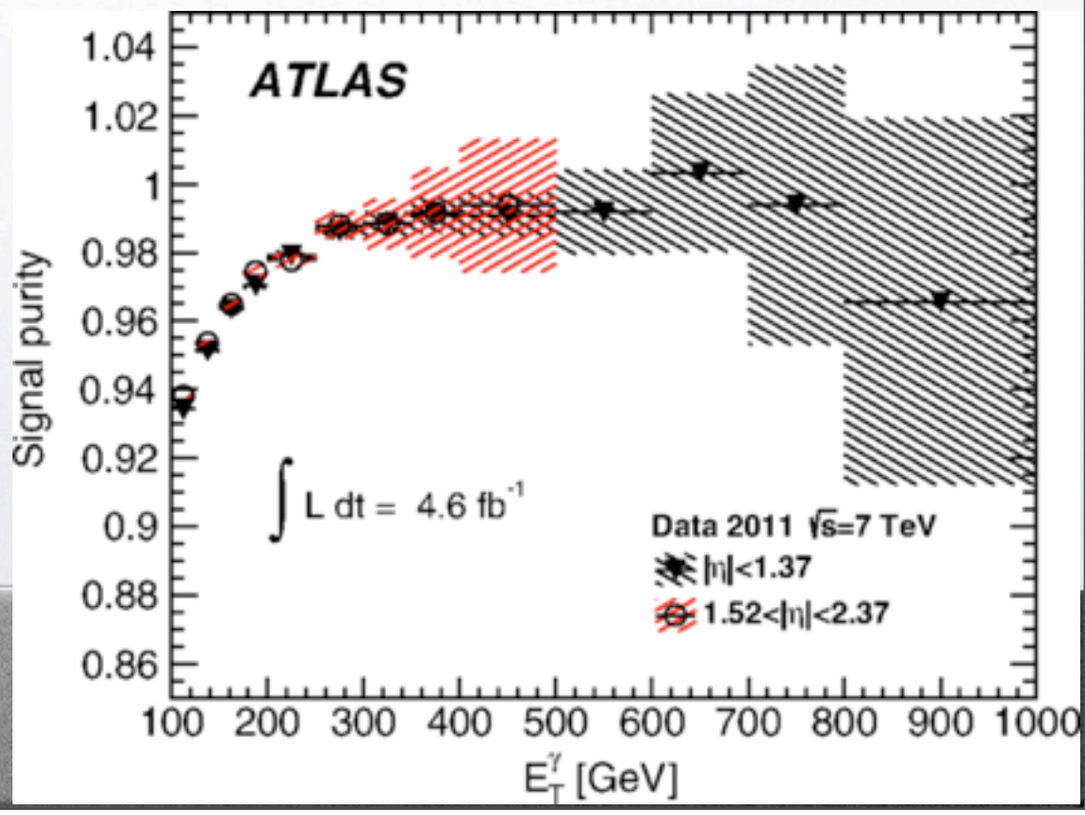

Photon performance

- Converted case results (complements slide 10 - unconverted).
- Also, consistent results for different methods : combined!

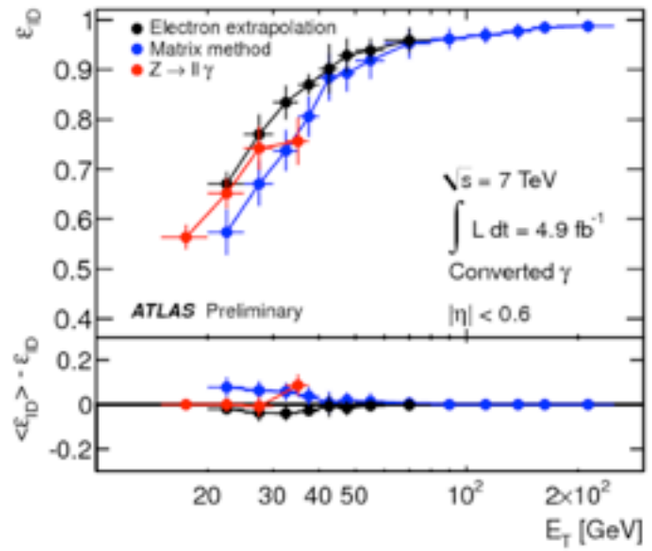

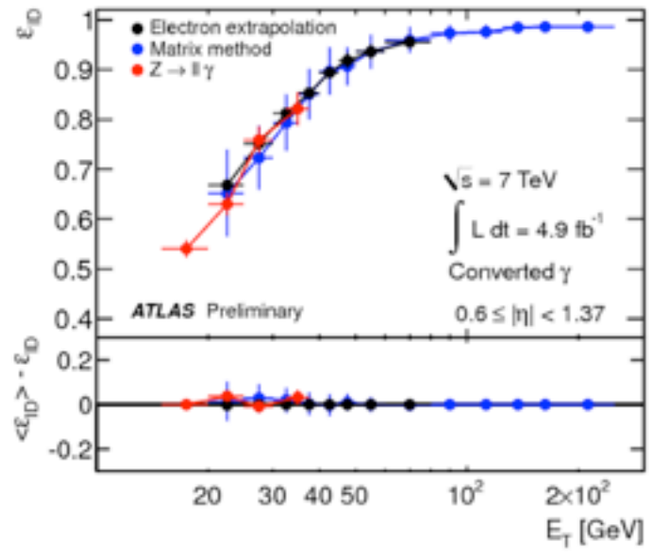

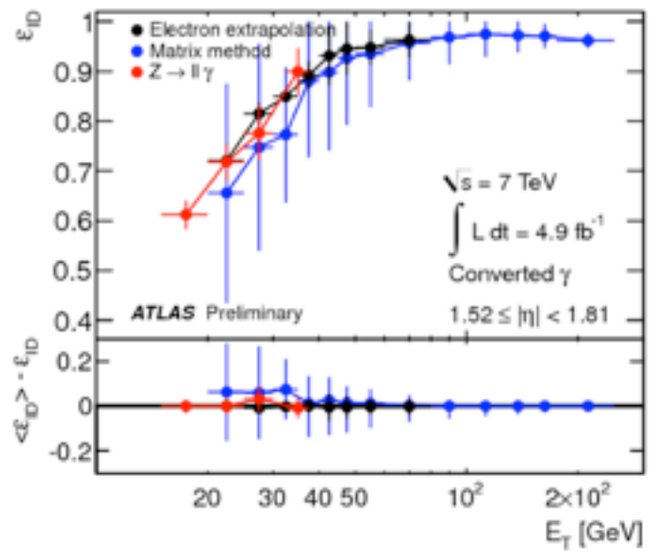

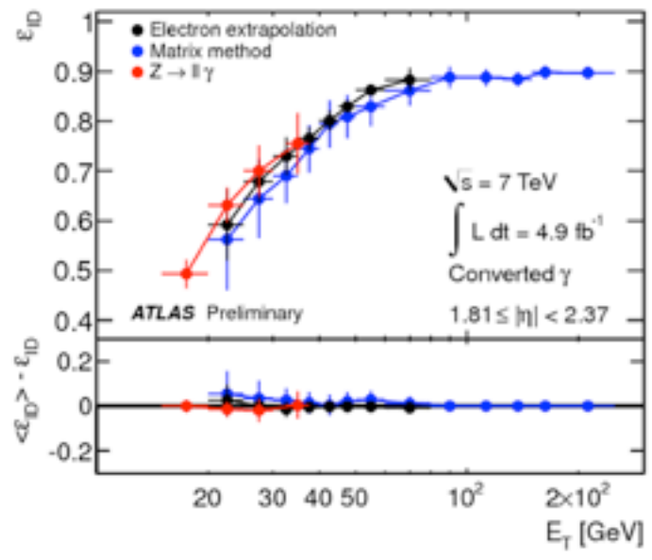

Electrons 2011/2012

- Demonstrating electron identification performance improvement on 2012 with respect to 2011.
- For tight cuts for the same nvtx variation a reduction of ~3.5% instead of ~6-7% on the losses related to pileup.

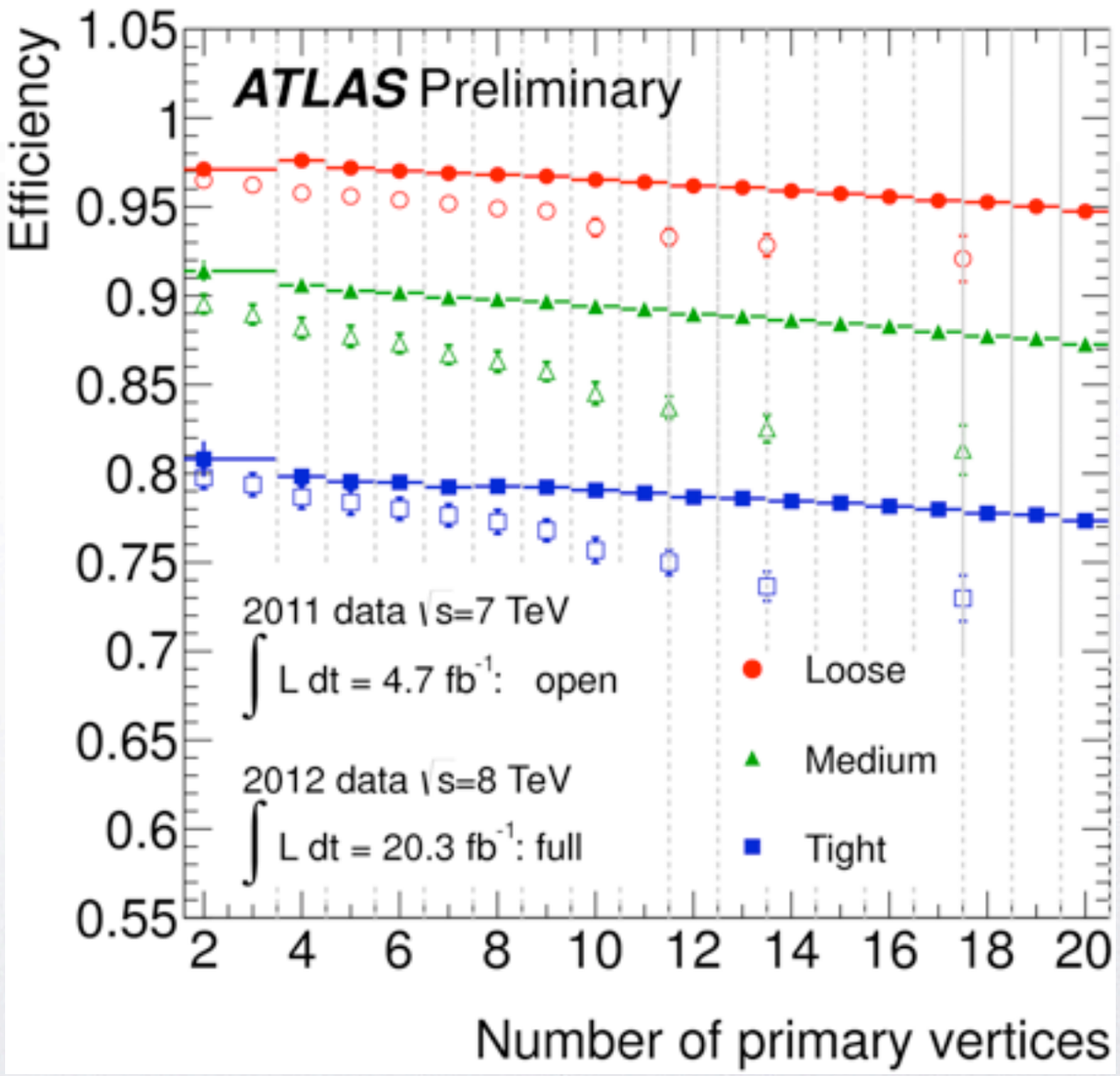

More improvements

- MVA-based calibration implemented. Calibration dependent on particle type (electron, unconverted or converted photon).
- Impact on resolution helps to improve performance also for H-> ɣ ɣ.
- detector description improved with data-driven estimates of material before the EM calorimeter.

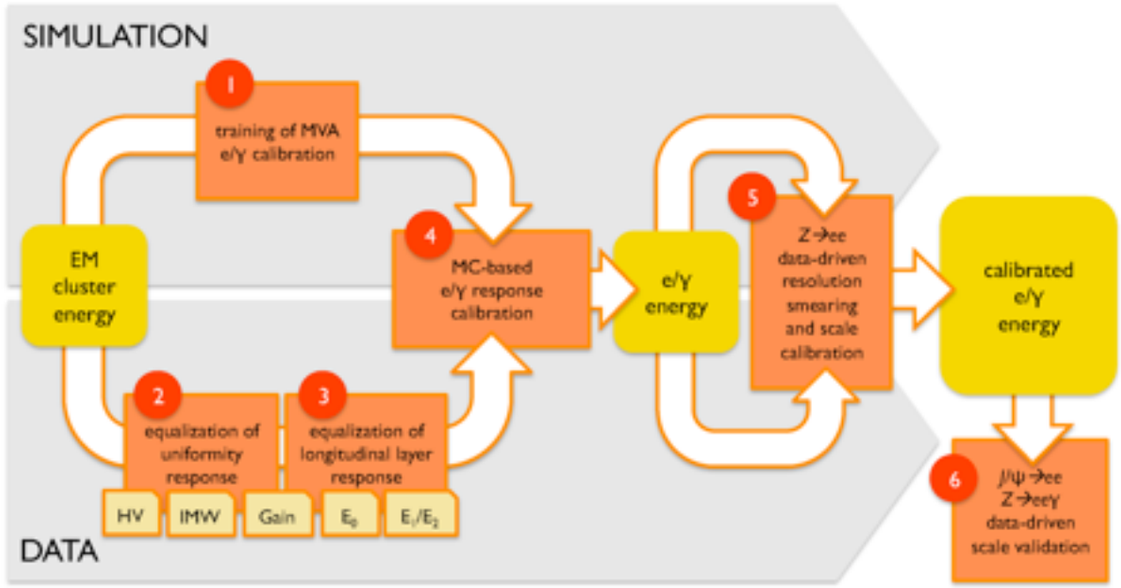

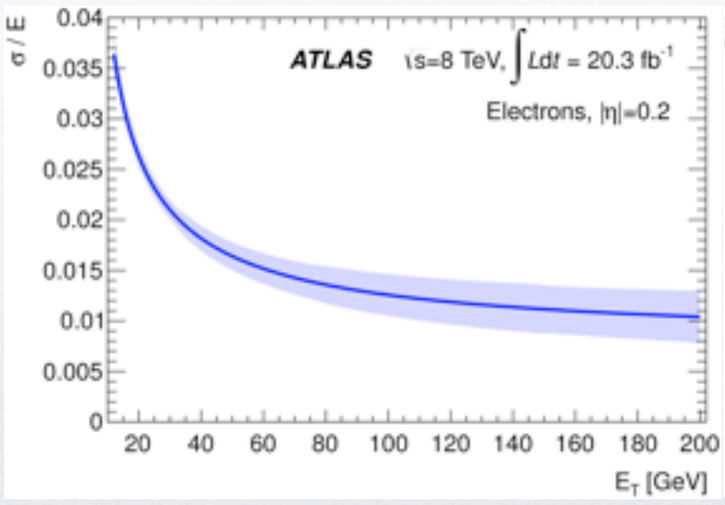

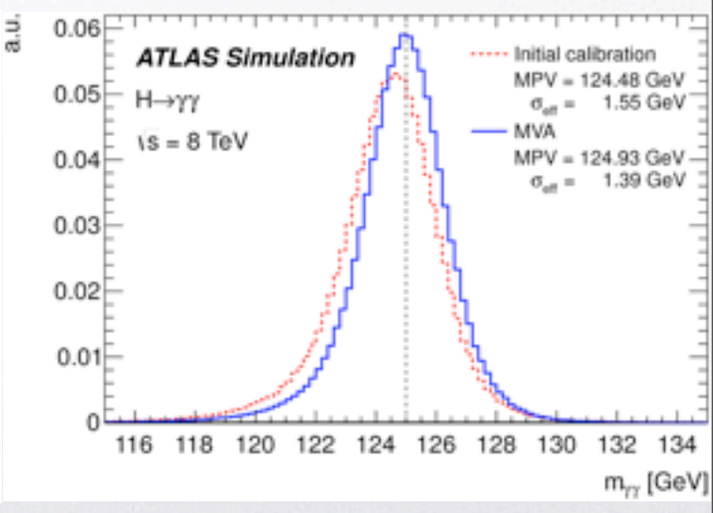

More on calibration

- New calibration improves data/MC correctness.
- Energy scale factors after applying a Z-based calibration. Band is the calibration systematic uncertainty, error bars represent the total uncertainty specific to the cross-checking analysis.

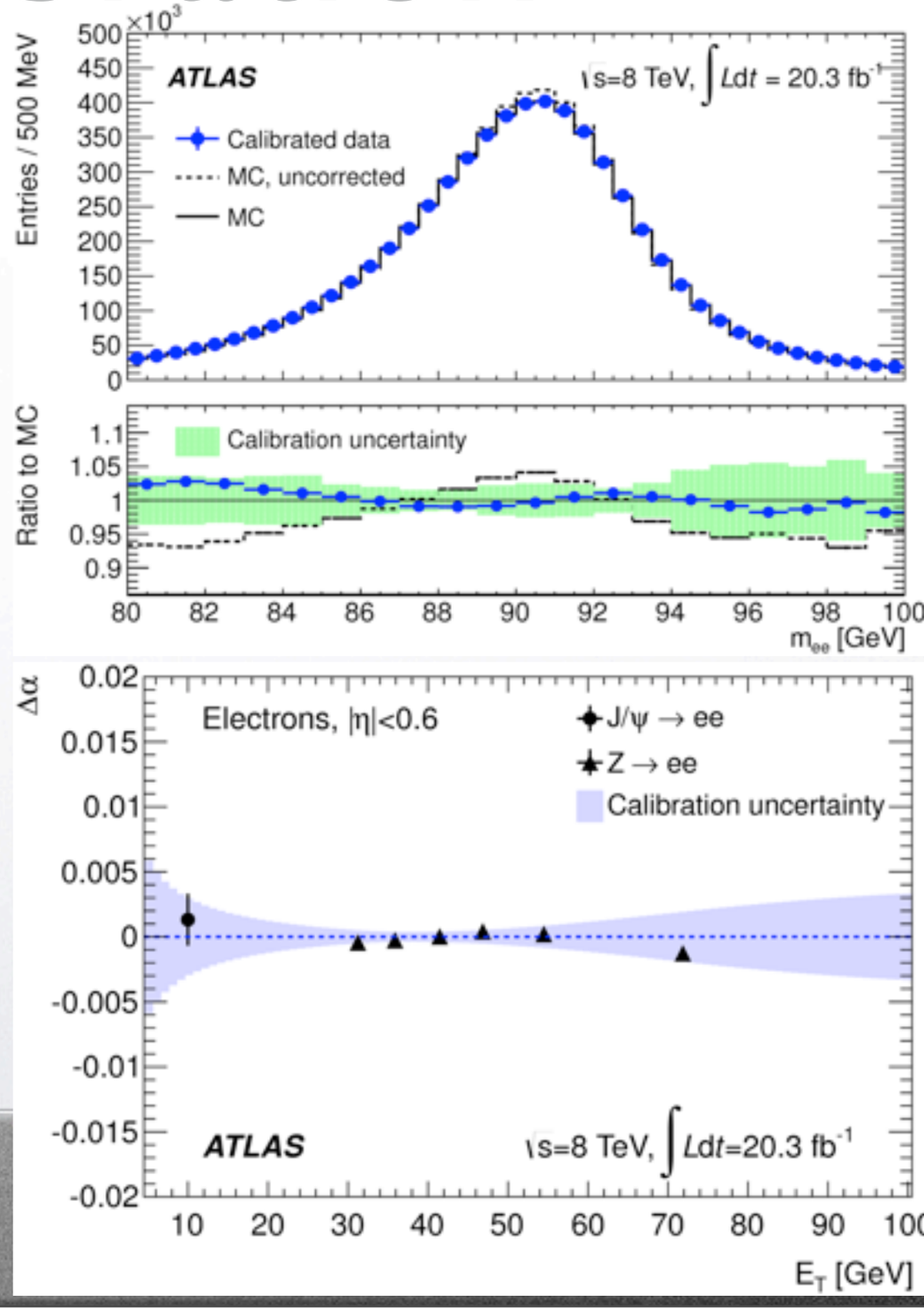

Identification variables

- All variables used for electron Identification in the central region (|η|<2.5).
- Unconverted photon ID variables are the Calorimeter one in this group.

Type	Description	Name
Hadronic leakage	Ratio of E_T in the first layer of the hadronic calorimeter to E_T of the EM cluster (used over the range $\|\eta\| < 0.8$ and $\|\eta\| > 1.37$)	R_{Had1}
	Ratio of E_T in the hadronic calorimeter to E_T of the EM cluster (used over the range $\|\eta\| > 0.8$ and $\|\eta\| < 1.37$)	R_{Had}
Third layer of EM calorimeter	Ratio of the energy in the third layer to the total energy	f_3
Middle layer of EM calorimeter	Lateral shower width, $\sqrt{(\Sigma E_i \eta_i^2)/(\Sigma E_i) - ((\Sigma E_i \eta_i)/(\Sigma E_i))^2}$, where E_i is the energy and η_i is the pseudorapidity of cell i and the sum is calculated within a window of 3×5 cells	$W_{\eta 2}$
	Ratio of the energy in 3×3 cells over the energy in 3×7 cells centered at the electron cluster position	R_ϕ
	Ratio of the energy in 3×7 cells over the energy in 7×7 cells centered at the electron cluster position	R_η
Strip layer of EM calorimeter	Shower width, $\sqrt{(\Sigma E_i (i - i_{\text{max}})^2)(\Sigma E_i)}$, where i runs over all strips in a window of $\Delta\eta \times \Delta\phi \approx 0.0625 \times 0.2$, corresponding typically to 20 strips in η, and i_{max} is the index of the highest-energy strip	W_{stot}
	Ratio of the energy difference between the largest and second largest energy deposits in the cluster over the sum of these energies	E_{ratio}
	Ratio of the energy in the strip layer to the total energy	f_1
	Shower width for three strips around strip with maximum energy deposit	w_{s3}
	Energy outside core of three central strips but within seven strips divided by energy within the three central strips	F_{side}
	Difference between the energy associated with the second maximum in the strip layer, and the energy reconstructed in the strip with the minimal value found between the first and second maxima	ΔE
Track quality	Number of hits in the B-layer (discriminates against photon conversions)	n_{Blayer}
	Number of hits in the pixel detector	n_{Pixel}
	Number of total hits in the pixel and SCT detectors	n_{Si}
	Transverse impact parameter	d_0
	Significance of transverse impact parameter defined as the ratio of d_0 and its uncertainty	σ_{d_0}
	Momentum lost by the track between the perigee and the last measurement point divided by original momentum	$\Delta p/p$
TRT	Total number of hits in the TRT	n_{TRT}
	Ratio of the number of high-threshold hits to the total number of hits in the TRT	F_{HT}
Track–cluster matching	$\Delta\eta$ between the cluster position in the strip layer and the extrapolated track	$\Delta\eta_1$
	$\Delta\phi$ between the cluster position in the middle layer and the extrapolated track	$\Delta\phi_2$
	Defined as $\Delta\phi_2$, but the track momentum is rescaled to the cluster energy before extrapolating the track to the middle layer of the calorimeter	$\Delta\phi_{\text{Res}}$
	Ratio of the cluster energy to the track momentum	E/p
Conversions	Veto electron candidates matched to reconstructed photon conversions	!isConv

Forward Electrons

- Variables used when no tracking is available.
- 2.5<|η|<4.9.

Category	Description	Variable
Acceptance	$2.5 < \|\eta\| < 4.9$	
Shower depth	Distance of the shower barycentre from the calorimeter front face measured along the shower axis	λ_{centre}
Maximum cell energy	Fraction of cluster energy in the most energetic cell	$f_{\max}$
Longitudinal second moment	Second moment of the distance of each cell to the shower centre in the longitudinal direction (λ_i)	$\langle\lambda^2\rangle$
Transverse second moment	Second moment of the distance of each cell to the shower centre in the transverse direction (r_i)	$\langle r^2\rangle$
Normalised lateral moment	w_2 and $w_{\max}$ are second moments of r_i for different weights per cell	$\frac{w_2}{w_2+w_{\max}}$
Normalised longitudinal moment	l_2 and $l_{\max}$ are the second moments of λ_i for different weights per cell	$\frac{l_2}{l_2+l_{\max}}$